Polyhedron xxx (2016) xxx–xxx

Contents lists available at ScienceDirect

Polyhedron

journal homepage: www.elsevier.com/locate/poly

Synthesis, characterization and reactivity of iron- and cobalt-pincer complexes

Ashleigh D. Smith, Anu Saini, Laci M. Singer, Neha Phadke, Michael Findlater *

Department of Chemistry & Biochemistry, Texas Tech University, Lubbock, TX 79409, USA

ARTICLE INFO

Article history:
Received 22 October 2015
Accepted 18 December 2015
Available online xxxx

Keywords:
Co complexes
Fe complexes
Pincer ligands
Solid state structures
Hydrosilylation

ABSTRACT

The ^{tBu}PONOP (2,6-bis(di-*tert*-butyl-phosphinito)pyridine) complexes of iron and cobalt, (^{tBu}PONOP)$FeCl_2$ (**1**) and (^{tBu}PONOP)$CoCl_2$ (**2**)) have been prepared. Both complexes are paramagnetic and the solid-state structures of **1** and **2** were determined by single crystal X-ray diffraction studies. Analogous Fe and Co complexes of the ^{tBu}PNP (2,6-bis(di-*tert*-butyl-phosphinomethyl)pyridine) ligand (**3** and **4**, respectively) were prepared to allow comparison between the closely related pincer ligands in the hydrosilylation of carbonyl moieties. All four complexes were found to be catalytically active when treated with $NaBEt_3H$, which was assumed to generate a metal-hydride species in-situ.

© 2016 Published by Elsevier Ltd.

1. Introduction

Pincer ligands have emerged as a privileged class of ligand in organometallic chemistry and have seen widespread use in catalysis [1–8]. In particular, Ir-based pincers have been shown to be effective catalysts in a range of valuable catalytic transformations [9–12]. Among these pincer ligands, neutral tridentate systems such as PNP and PONOP have emerged as leading platforms for the study of catalytic reactions [13,14]. Given the high cost of precious metals such as Ir and Rh, the application of such ligands in base metal catalysis is no surprise and a number of reports have appeared in which such base–metal complexes were deployed in fields ranging from energy science to asymmetric catalysis [15,16].

Given our interest in the hydrosilylation of carbonyl moieties using iron [17], we turned our attention to the synthesis and reactivity of first-row metal PONOP and PNP pincer complexes. These types of PONOP and PNP ligands are readily available via salt metathesis reactions between 2,6-dihydroxypyridines or 2,6-bis (bromomethyl)pyridines and dichlorophosphines to afford either PONOP or PNP pincer ligands, respectively. As befitting the status of a privileged class of ligands, the modular fashion in which they can be synthesized allows versatility in ligand platform design that is virtually unmatched. Given such versatility, it is surprising that only a few Fe- and Co-PONOP and PNP pincer complexes have been reported in the literature, although related systems have also been disclosed. An overview of cobalt and iron PNP and PONOP pincer systems, is depicted in Scheme 1 [18–26]. It should be noted that several related iron and cobalt complexes containing anionic pincer-type PCP, POCOP, and PN^{pyrrole}P frameworks have been described [27–33].

In this report, the synthesis, characterization, and reactivity of new (PONOP)M (M = Fe and Co) complexes are examined. Reactions of these metal PONOP complexes with $NaBEt_3H$ result in catalytically competent systems for the hydrosilylation of carbonyl groups. The synthesis and characterization of the, presumably, metal hydride complexes proved to be difficult because of the instability of these complexes, even at room temperature under inert atmosphere.

2. Results and discussion

Treatment of anhydrous $FeCl_2$ or $CoCl_2$ with the ligand tBuPONOP in THF affords the 16*e* and 17*e* complexes (^{tBu}PONOP)$FeCl_2$ (**1**) and (^{tBu}PONOP)$CoCl_2$ (**2**), respectively, in low yields after crystallization (Scheme 2). Both complexes exhibit broad NMR resonances consistent with paramagnetic compounds. Single crystals of both **1** and **2** were grown from concentrated toluene solutions at low temperature and analyzed by X-ray crystallography. The solid-state structures of **1** and **2** are shown in Fig. 1.

As we were preparing our manuscript, Schrodi and coworkers disclosed the solid-state structure of complex **1**.[26] However, significant differences exist between the two structures. In our hands, **1** crystallized in the monoclinic space group rather than the previously reported triclinic system. Overall, the geometry is consistent with the previously reported crystal structure and with the

* Corresponding author.
E-mail address: michael.findlater@ttu.edu (M. Findlater).

http://dx.doi.org/10.1016/j.poly.2015.12.037
0277-5387/© 2016 Published by Elsevier Ltd.

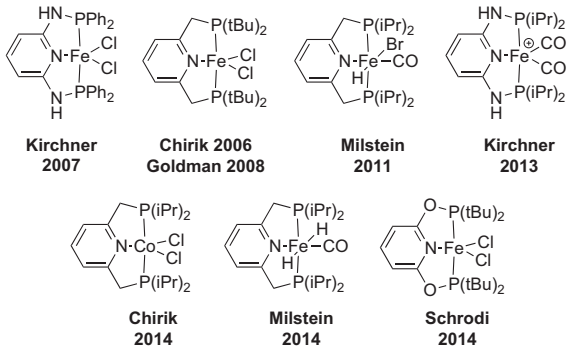

Scheme 1. Overview of Fe/Co PNP and PONOP complexes reported in the literature.

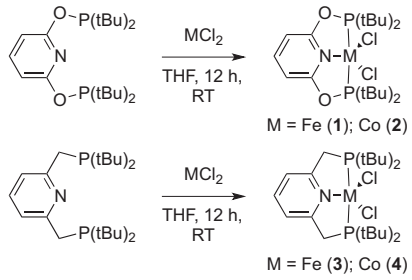

Scheme 2. Synthesis of (PONOP)M and (PNP)M complexes.

analogous structure, (^{tBu}PNP)FeCl$_2$ (**3**) [34]. However, the geometry around the iron center is best described as a *distorted* square pyramid with one chloride in the apical position and the nitrogen of the pyridine ring, the two phosphorus atoms and the remaining chlorine forming the basal plane. The structural distortion in complex **1** arises from an iron center, which is raised above the basal plane by a distance of 0.433 Å. The Fe–Cl(1) and Fe–Cl(2) distances are very different, 2.365(2) and 2.268(2) Å, respectively. Similarly, N–Fe–Cl(1) and N–Fe–Cl(2) bond angles are also dissimilar, 136.4(3)° and 117.1(3)°, respectively. Close examination of the packing diagram reveals the cause to be the presence of secondary bonding interactions between the chloride ligands and adjacent ligand-based H-atoms (Fig. 1b). Curiously, a bifurcated non-bonding interaction is present involving both chlorides and a second interaction is observed only with Cl(1). This additional secondary bonding interaction accounts for the lengthening of the Fe–Cl(1) bond distance.

The solid-state structure of **2** (Fig. 1c) is essentially isostructural with that of **1**, only less distorted. Like **1**, analysis of the bonding in **2** unearths inequivalent cobalt-chloride bond lengths for the apical and the basal sites (2.389(1) and 2.253(1) Å, respectively). Once more, N–Co–Cl(1) and N–Co–Cl(2) bond angles also vary widely, 97.94(7)° and 160.72(8)°, respectively. We attributed the distortions from ideal square pyramidal geometry in **1** to intermolecular non-bonding interactions. As anticipated, upon examination of the extended packing of **2** we observed a similar network of intermolecular interactions (Fig. 1d). Thus, the presence of non-bonding interactions between the chloride ligands and adjacent ligand-based H-atoms is revealed. However, unlike **1** there are no 'chelating' interactions between both chloride ligands and an adjacent

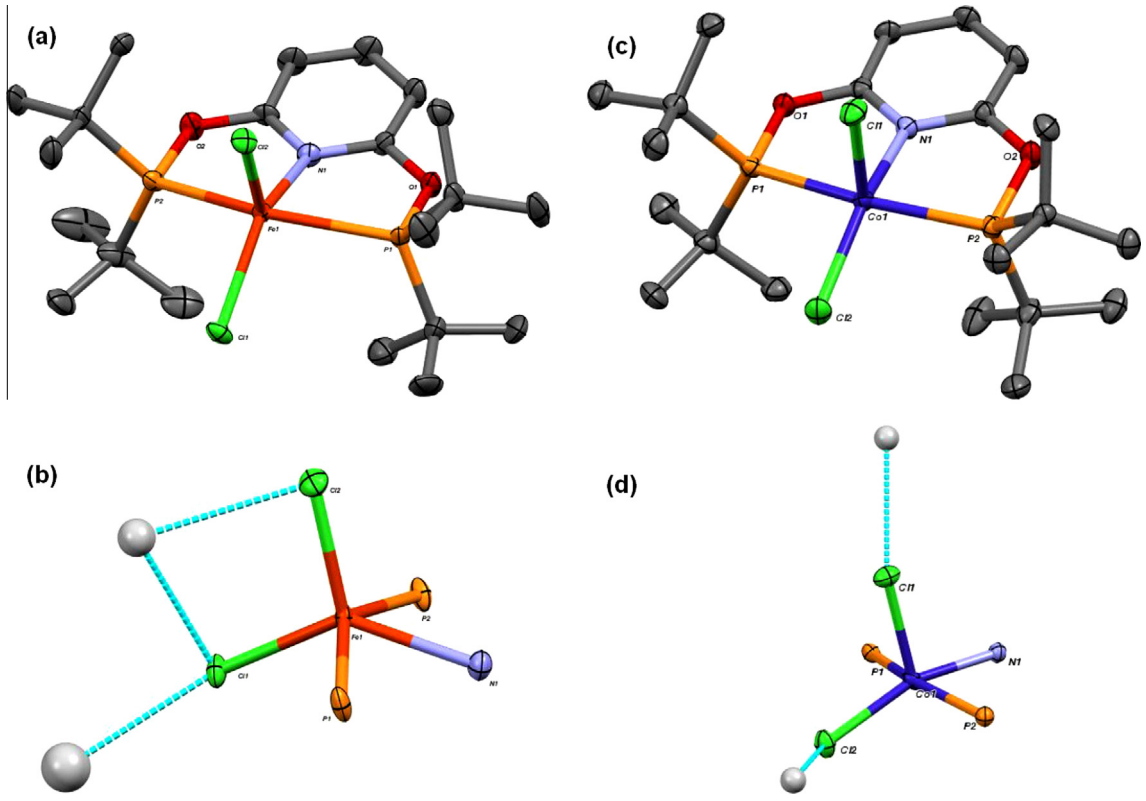

Fig. 1. (a) Solid-state structure of **1**. Hydrogen atoms omitted for clarity. Thermal ellipsoids at 30% probability. Key bond lengths (Å) and bond angles (°): N1–Fe1 2.268(8), P1–Fe1 2.526(2), P2–Fe1 2.503(2), Fe1–Cl1 2.365(2), Fe–Cl2 2.268(2), P1–Fe1–P2 144.68(8), N1–Fe1–Cl1 136.4(3), N1–Fe1–Cl2 117.1(3), Cl1–Fe1–Cl2 106.53(7). (b) H-bonding contacts to chloride ligands account for distortion of square–pyramidal metal center geometry. (c) Solid-state structure of **2**. Hydrogen atoms omitted for clarity. Thermal ellipsoids at 30% probability. Key bond lengths (Å) and bond angles (°): N1–Co1 1.971(2), P1–Co1 2.281(1), P2–Co1 2.277(1), Co1–Cl1 2.389(1), Co1–Cl2 2.253(1), P1–Co1–P2 160.38(3), N1–Co1–Cl1 97.94(7), N1–Co1–Cl2 160.72(8), Cl1–Co1–Cl2 101.34(3). (d) H-bonding contacts to chloride ligands account for distortion of square–pyramidal metal center geometry.

Please cite this article in press as: A.D. Smith et al., Polyhedron (2016), http://dx.doi.org/10.1016/j.poly.2015.12.037

Download English Version:

https://daneshyari.com/en/article/7764561

Download Persian Version:

https://daneshyari.com/article/7764561

Daneshyari.com